Article

MMS

Mathematics and Mechanics of Solids
16(8): 872–886

DOI: 10.1177/1081286511401364
mms.sagepub.com
SAGE

Mechanics of membrane–membrane adhesion

Ashutosh Agrawal

Department of Applied Physics, California Institute of Technology, Pasadena, CA, USA

Received 10 January 2011; accepted 27 January 2011

Abstract
Curvature elasticity is used to derive the equilibrium conditions that govern the mechanics of membrane–membrane adhesion. These include the Euler–Lagrange equations and the interface conditions which are derived here for the most general class of strain energies permissible for fluid surfaces. The theory is specialized for homogeneous membranes with quadratic 'Helfrich'-type energies with non-uniform spontaneous curvatures. The results are employed to solve four-point boundary value problems that simulate the equilibrium shapes of lipid vesicles that adhere to each other. Numerical studies are conducted to investigate the effect of relative sizes, osmotic pressures, and adhesion-induced spontaneous curvature on the morphology of adhered vesicles.

Keywords
interface conditions, lipid membranes, membrane–membrane adhesion

1. Introduction

Adhesion plays a significant role in cell physiology affecting numerous processes such as cellular transport, cell motility and signal transduction. Although real biological systems exhibit a complex interplay among cell membranes, proteins and cytoskeleton, simple quantitative models can provide key insights into the underlying mechanisms. As the lipid membranes form the interface of cells and its various organelles, adhesion of membranes has been a subject of considerable interest in the literature. However, this has mainly been limited to the adhesion of membranes to rigid structures [1–8]. These studies have provided vital insights into the morphological transformations that the lipid vesicles undergo due to adhesion with planar and curved substrates. In the context of cellular biology, however, membrane–membrane adhesion is more relevant and ubiquitous, the most common phenomenon being cell–cell adhesion. Adhesion of lipid vesicles with cell membrane regulates inter- and intra-cellular transport including transmission of electric signals at synapses in neurons [9]. Furthermore, membrane–membrane interactions can be expected to play an important role in the transport of flexible nanocarriers such as liposomes into cells that are employed for the purposes of therapeutics and diagnostics.

Membrane–membrane adhesion has been studied for homogeneous lipid membranes with Helfrich-type energy [6, 10–12]. Evans [10] used a force-balance approach to obtain the equilibrium conditions. The effect of adhesion was incorporated into the model as a distributed stress that acts in a direction normal to the contact domain. The model was developed under two assumptions: (i) the contact domain was considered to be a

Corresponding author:
Ashutosh Agrawal, Department of Applied Physics, California Institute of Technology, Pasadena, CA 91125, USA.
Email: aagrawal@caltech.edu

planar surface; and (ii) the normal curvature of the contact boundary in the tangential direction was assumed to vanish. Derganc et al. [11] employed the area difference elasticity model to derive the Euler–Lagrange equations and the edge conditions for adhering membrane domains exhibiting axisymmetry. The results were employed to model the shapes of identical erythrocytes that aggregate to form a long rouleau. To this end, periodic boundary conditions were invoked that required the integration of governing differential equations over two membrane domains. Interface conditions for adhering membranes with quadratic energy and vanishing spontaneous curvature that exhibit arbitrary morphology were derived by Muller et al. [6]. Ziherl and Svetina [12] used the area difference elasticity model to simulate vesicle–vesicle adhesion. In contrast to Derganc et al., direct minimization of the total free energy of the system was performed using Surface Evolver [13] to obtain the equilibrium shapes of the adhered vesicles.

In this work we extend these previous studies to achieve two objectives. First, we derive the equilibrium conditions for membrane–membrane adhesion in the most generalized setting permissible for a fluid shell. The model allows for the incorporation of higher order curvature terms in the energy functional. It also accommodates spatially non-uniform membrane properties and adhesion energy. Second, we model vesicle–vesicle adhesion that necessitates integration of the governing differential equations concurrently over three domains. These simulations are of a more general nature than those previously carried out to model vesicle–substrate adhesion and rouleau formation. We employ the generalized framework to model the equilibrium shapes of vesicles for the cases when the adhesion molecules can possibly induce spontaneous curvature in the contact domain. This interaction is similar to that considered by Lipowsky [14] where polymer chains anchored to membrane surfaces induced a preferential curvature.

The paper is structured as follows. In Section 2, we briefly review the geometric framework and the potential energy associated with a lipid membrane. In Section 3, we set up the problem for modeling membrane–membrane adhesion. The effect of adhesion is incorporated via a phenomenological energetic term proportional to the area of contact. We thus adopt a coarse-grained approach that indirectly takes into consideration the effect of intermolecular forces due to van der Waals forces, electrostatic interactions and binding of adhesion proteins. Equilibrium conditions are derived for the free domains and the contact domain. Boundary working terms from all of the domains are combined to obtain the generalized interface conditions at the periphery of the adhered domain. The results are then specialized for homogeneous membranes with Helfrich-type strain energy in Section 4. Finally, in Section 5 we employ the derived results to simulate the equilibrium morphology of two vesicles adhered to each other. Equilibrium shapes are obtained for vesicles with different sizes, osmotic pressures and spontaneous curvature in the adhered domain.

2. Geometry and potential energy of a lipid membrane

Let ω be a two-dimensional surface parametrized by coordinates θ^μ ($\mu = 1, 2$) and $\mathbf{r}(\theta^\mu)$ be the position vector to any point on the surface. This yields the basis vectors $\mathbf{a}_\alpha = \mathbf{r}_{,\alpha}$ and the metric $a_{\alpha\beta} = \mathbf{a}_\alpha \cdot \mathbf{a}_\beta$. The local orientation at a point is given by the unit surface normal $\mathbf{n} = \mathbf{a}_1 \times \mathbf{a}_2 / |\mathbf{a}_1 \times \mathbf{a}_2|$. Surface tensor $\mathbf{b} = b_{\alpha\beta}\mathbf{a}^\alpha \otimes \mathbf{a}^\beta$ with covariant components

$$b_{\alpha\beta} = \mathbf{n} \cdot \mathbf{r}_{,\alpha\beta} = -\mathbf{a}_\alpha \cdot \mathbf{n}_{,\beta} \tag{1}$$

furnishes the local curvatures. Here and henceforth, $()_{,\alpha} = \partial()/\partial\theta^\alpha$. Using a pair of orthonormal vectors $\boldsymbol{\nu}$ and $\boldsymbol{\tau}$ on the tangent plane, the curvature tensor can be expressed as

$$\mathbf{b} = \kappa_\nu\, \boldsymbol{\nu} \otimes \boldsymbol{\nu} + \kappa_\tau\, \boldsymbol{\tau} \otimes \boldsymbol{\tau} + \tau\, (\boldsymbol{\nu} \otimes \boldsymbol{\tau} + \boldsymbol{\tau} \otimes \boldsymbol{\nu}), \tag{2}$$

where τ is the twist and $\{\kappa_\nu, \kappa_\tau\}$ are the normal curvatures associated with $\boldsymbol{\nu}$ and $\boldsymbol{\tau}$, respectively. They are given by

$$\kappa_\nu = b_{\alpha\beta}\nu^\alpha\nu^\beta, \quad \kappa_\tau = b_{\alpha\beta}\tau^\alpha\tau^\beta \quad \text{and} \quad \tau = b_{\alpha\beta}\nu^\alpha\tau^\beta. \tag{3}$$

Equations (2) and (3) can be combined to obtain the two invariants of the curvature tensor, namely, the mean curvature

$$H = \tfrac{1}{2}\,\mathrm{tr}\,\mathbf{b} = \tfrac{1}{2}(\kappa_\nu + \kappa_\tau), \tag{4}$$

and the Gaussian curvature

$$K = \det \mathbf{b} = \kappa_\nu \kappa_\tau - \tau^2. \tag{5}$$

Owing to its flexural stiffness and diffusivity of lipid molecules, a biomembrane behaves as a fluid shell. For a thin elastic shell, the strain energy depends on the surface strain tensor and surface curvature tensor. An elastic shell exhibits a fluid behavior if the strain energy remains invariant under any in-plane shear deformation. This generates a symmetry restriction analogous to that introduced by Noll for simple fluids in a three-dimensional setting and requires the areal strain energy functional W to have the canonical form [15]

$$W = W(\rho, H, K; \theta^\mu), \tag{6}$$

where ρ is the areal density. For a surface ω, the potential energy is thus given by

$$E = \int_\omega W(\rho, H, K; \theta^\mu)\, da. \tag{7}$$

A constraint on the surface area and the enclosed volume is imposed by constructing the augmented energy functional

$$E = \int_\omega [W(H, K; \theta^\alpha) + \lambda(\theta^\alpha)]\, da - pV, \tag{8}$$

where λ and p are the Lagrange multipliers associated with the area and the volume constraint, respectively; V is the total volume enclosed by the surface ω and can be expressed as

$$V = \int_\omega \tfrac{1}{3}\mathbf{r} \cdot \mathbf{n}\, da. \tag{9}$$

Minimization of E in (8) yields the Euler–Lagrange equations and the boundary conditions necessary to obtain equilibrium configurations of a membrane surface.

3. Membrane–membrane adhesion

We now consider two membrane surfaces ω_1 and ω_2 that adhere over a subdomain ω_c with the boundary $\partial\omega_c$. Let $\tilde{\omega}_1$ and $\tilde{\omega}_2$ be the free domains associated with ω_1 and ω_2, respectively, such that $\omega_1 = \tilde{\omega}_1 \cup \omega_c$ and $\omega_2 = \tilde{\omega}_2 \cup \omega_c$ (Figure 1). We assume that the surface normals $\mathbf{n}_1$ and $\mathbf{n}_2$ to the two surfaces are continuous everywhere including the boundary $\partial\omega_c$. This keeps the curvature and, hence, the bending energy bounded. The positive directions of the surface normals are chosen such that the two normals are aligned in the same direction at the interface. If ω_1 and ω_2 are the surfaces of two closed vesicles, then the above sign convention leads to one outward and one inward acting normal for the two vesicles. In the contact region, we align the common normal to the surface $\mathbf{n}_c$ with $\mathbf{n}_1$ and $\mathbf{n}_2$. The adhesion interaction is accounted by incorporating a phenomenological energy

$$E_a = -\int_{\omega_c} \sigma(\theta^\alpha)\, da, \tag{10}$$

where $\sigma(\theta^\alpha)$ is the adhesion energy per unit area that can accommodate explicit dependence on surface coordinates permitting non-homogeneous interactions. A positive σ lowers the system energy thereby promoting adhesion.

Let $W^1(H, K; \theta^\alpha)$ and λ_1 be the strain energy function and surface tension in ω_1. Similarly, let $W^2(H, K; \theta^\alpha)$ and λ_2 be the corresponding quantities for ω_2. For closed membrane structures, such as lipid vesicles, let $\tilde{p}_1$ and $\tilde{p}_2$ be the internal pressures experienced by ω_1 and ω_2. If we assume $\mathbf{n}_1$ to be an outward acting normal to ω_1 and $\mathbf{n}_2$ to be an inward acting normal to ω_2, for an external pressure $\tilde{p}_o$ exerted by the surrounding environment onto the two surfaces, the net transmembrane pressures acting on the free domains $\tilde{\omega}_1$ and $\tilde{\omega}_2$ in the direction

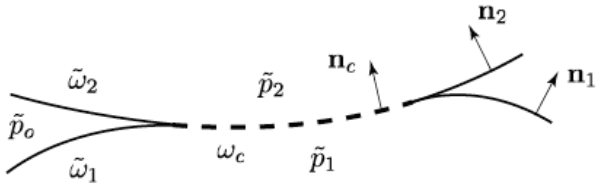

Figure 1. Adhesion between two lipid membranes over the surface ω_c.

of their respective surface normals are given by $p_1 = \tilde{p}_1 - \tilde{p}_o$ and $p_2 = \tilde{p}_o - \tilde{p}_2$. For the case of constrained surface area and enclosed volume, the total free energy of the system can be written as

$$E = \int_{\omega_1} [W^1(H,K;\theta^\alpha) + \lambda_1(\theta^\alpha)]\, da - p_1 \int_{\omega_1} \tfrac{1}{3}\mathbf{r}\cdot\mathbf{n}_1\, da + \int_{\omega_2} [W^2(H,K;\theta^\alpha) + \lambda_2(\theta^\alpha)]\, da$$
$$-p_2 \int_{\omega_2} \tfrac{1}{3}\mathbf{r}\cdot\mathbf{n}_2\, da - \int_{\omega_c} \sigma(\theta^\alpha) da. \tag{11}$$

Here we have assumed that the two surfaces can freely slide past each other without any frictional resistance.

The energy functional in (11) can be expressed as the sum of energies associated with the two free domains $\tilde{\omega}_1$ and $\tilde{\omega}_2$ and the contact domain $\tilde{\omega}_c$. This yields

$$E = E_1 + E_2 + E_c, \tag{12}$$

where

$$E_i = \int_{\tilde{\omega}_i} [W^i(H,K;\theta^\alpha) + \lambda_i(\theta^\alpha)]\, da - p_i \int_{\tilde{\omega}_i} \left(\tfrac{1}{3}\mathbf{r}\cdot\mathbf{n}_i\right)\, da \tag{13}$$

is the free energy associated with the free surface $\tilde{\omega}_i$ ($i = \{1,2\}$), and

$$E_c = \int_{\omega_c} [W^1(H,K;\theta^\alpha) + W^2(H,K;\theta^\alpha) + \lambda_1(\theta^\alpha) + \lambda_2(\theta^\alpha)]\, da - \int_{\omega_c} (p_1+p_2)\left(\tfrac{1}{3}\mathbf{r}\cdot\mathbf{n}_c\right)\, da - \int_{\omega_c} \sigma(\theta^\alpha)\, da \tag{14}$$

is the combined energy of the contact domain.

3.1. Free domains

To compute the variation of the augmented energy functional, we consider a family of surfaces generated by $\mathbf{r}(\theta^\alpha;\epsilon)$ where ϵ is a parameter and $\mathbf{r}(\theta^\alpha) = \mathbf{r}(\theta^\alpha;\epsilon)\ |_{\epsilon=0}$ yields the equilibrium configuration. The virtual displacement is then given by

$$\mathbf{u}(\theta^\alpha) = \tfrac{\partial}{\partial\epsilon}\mathbf{r}(\theta^\alpha;\epsilon)_{|\epsilon=0} = \dot{\mathbf{r}},$$

where the dot refers to the derivative with respect to the parameter ϵ.

First, we consider variation of the energy functional E_i associated with the free domains. Using (13), the variation of E_i induced by $\mathbf{u}$ is obtained as

$$\dot{E}_i = \int_{\tilde{\omega}_i} [\dot{W}^i + (W^i + \lambda_i)\dot{J}/J]\, da - p_i \left(\int_{\tilde{\omega}_i} \tfrac{1}{3}\mathbf{r}\cdot\mathbf{n}_i\, da\right)^{\cdot}, \tag{15}$$

where

$$\dot{W}^i = W^i_H \dot{H} + W^i_K \dot{K} \tag{16}$$

and the subscripts H and K refer to partial derivatives with respect to these variables.

Any general variation $\mathbf{u}$ can be decomposed into

$$\mathbf{u} = u^\alpha \mathbf{a}_\alpha + u\mathbf{n}, \tag{17}$$

where u^α and u are, respectively, the tangential and the normal components of the variations. Following the procedure outlined in [16], tangential variations yield

$$\dot{J}/J = u^\alpha_{;\alpha}, \quad \dot{H} = u^\alpha H_{,\alpha} \quad \text{and} \quad \dot{K} = u^\alpha K_{,\alpha}. \tag{18}$$

These combined with (15), (16), and the fact that the last term in (15) vanishes for tangential variations furnish

$$\dot{E}_i = \int_{\tilde{\omega}_i} u^\alpha (W^i_H H_{,\alpha} + W^i_K K_{,\alpha} - W^i_{,\alpha} - (\lambda_i)_{,\alpha})\, da + \int_{\partial\tilde{\omega}_i} (W^i + \lambda_i) u^\alpha \nu^i_\alpha \, ds, \tag{19}$$

where $\boldsymbol{\nu}_i = \boldsymbol{\tau}_i \times \mathbf{n}_i$ is the exterior normal to the boundary $\partial\tilde{\omega}_i$ in the tangent plane and $\boldsymbol{\tau}_i$ is the tangent to the boundary in the direction of increasing arclength. Figure 2 shows the tangent and the normal vectors to a boundary $\partial\omega$ on an arbitrary surface ω. As W^i is assumed to be a function of H, K, and θ^α,

$$W^i_{,\alpha} = W^i_H H_{,\alpha} + W^i_K K_{,\alpha} + \partial W^i/\partial\theta^\alpha. \tag{20}$$

Substitution of (20) in (19) yields the Euler equation [17]

$$(\lambda_i)_{,\alpha} = -\partial W^i/\partial\theta^\alpha. \tag{21}$$

For a lipid bilayer with uniform properties, the strain energy has no explicit dependence on θ^α and the right-hand side of (21) reduces to zero. This leads to the familiar case usually encountered in the literature where the surface tension assumes a constant value over the entire surface. On the other hand, if the lipid bilayer has non-homogeneous properties, such as a variable spontaneous curvature or a variable bending modulus, due to biochemical interactions with proteins or lipids of varying geometry, the surface tension field varies spatially and is given by (21).

For normal variations [16],

$$\dot{J}/J = -2Hu, \quad 2\dot{H} = \Delta u + u(4H^2 - 2K) \quad \text{and} \quad \dot{K} = 2KHu + (\tilde{b}^{\alpha\beta} u_{,\alpha})_{;\beta}, \tag{22}$$

where $\Delta(\cdot) = a^{\alpha\beta}(\cdot)_{;\alpha\beta}$ is the surface Laplacian and $\tilde{b}^{\alpha\beta} = \varepsilon^{\alpha\lambda}\varepsilon^{\beta\gamma} b_{\lambda\gamma}$ is the contravariant cofactor of the curvature tensor. As shown in [18], variation of the volumetric term in (15) is given by

$$\left(\int_{\tilde{\omega}_i} \left(\tfrac{1}{3}\mathbf{r}\cdot\mathbf{n}_i\right)\, da \right)^{\cdot} = \int_{\tilde{\omega}_i} u\, da. \tag{23}$$

This together with (21), (22) and some rearrangements yield

$$\begin{aligned} \dot{E}_i = \int_{\tilde{\omega}_i} u \left[\Delta\left(\frac{1}{2} W^i_H\right) + (W^i_K)_{;\beta\alpha}\tilde{b}^{\beta\alpha} + W^i_H(2H^2 - K) + 2KHW^i_K - 2H(W^i + \lambda_i) - p_i \right] da \\ + \int_{\partial\tilde{\omega}_i} \left[\frac{1}{2} W^i_H \nu^\alpha_i u_{,\alpha} - \frac{1}{2}(W^i_H)_{,\alpha}\nu^\alpha_i u + W^i_K \tilde{b}^{\alpha\beta}\nu^i_\beta u_{,\alpha} - (W^i_K)_{,\alpha}\tilde{b}^{\alpha\beta}\nu^i_\beta u \right] ds, \end{aligned} \tag{24}$$

Above, ν^i_α and ν^α_i are the covariant and the contravariant components of $\boldsymbol{\nu}_i$, respectively. Equation (24) furnishes the second Euler equation

$$\Delta\left(\frac{1}{2} W^i_H\right) + (W^i_K)_{;\beta\alpha}\tilde{b}^{\beta\alpha} + W^i_H(2H^2 - K) + 2KHW^i_K - 2H(W^i + \lambda_i) = p_i \quad \text{on } \tilde{\omega}_i. \tag{25}$$

With (21) and (25) satisfied in the domain $\tilde{\omega}_i$, the variation of the energy reduces to the boundary term [19]

$$\dot{E}^B_i = \int_{\partial\tilde{\omega}_i} (W^i + \lambda_i) u^\alpha \nu^i_\alpha \, ds + \int_{\partial\tilde{\omega}_i} \left[\frac{1}{2} W^i_H \nu^\alpha_i u_{,\alpha} - \frac{1}{2}(W^i_H)_{,\alpha}\nu^\alpha_i u + W^i_K \tilde{b}^{\alpha\beta}\nu^i_\beta u_{,\alpha} - (W^i_K)_{,\alpha}\tilde{b}^{\alpha\beta}\nu^i_\beta u \right] ds, \tag{26}$$

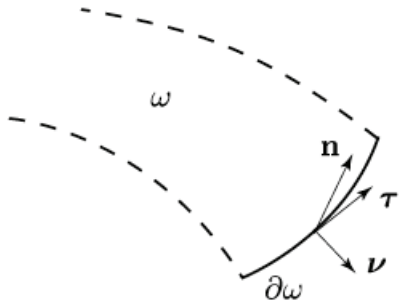

Figure 2. An arbitrary membrane domain ω with a boundary $\partial\omega$ and the associated orthonormal vectors $\mathbf{n}$, $\boldsymbol{\nu}$ and $\boldsymbol{\tau}$.

where the two integrals are the contributions from the tangential and the normal variations, respectively.

Following the elaborate procedure outlined in [19], the above equation can be expressed in a more tractable form. Here, we briefly review the key steps. Employing the definitions of $\boldsymbol{\nu}_i$ and $\boldsymbol{\tau}_i$, the derivative $u_{,\alpha}$ can be expressed as

$$u_{,\alpha} = \tau^i_\alpha u_{,\tau_i} + \nu^i_\alpha u_{,\nu_i}, \tag{27}$$

where $u_{,\tau_i}$ and $u_{,\nu_i}$ are the directional derivatives of the normal variation along the tangent $\boldsymbol{\tau}_i$ and the normal $\boldsymbol{\nu}_i$ to the edge. Recalling the facts that $u = \mathbf{u}\cdot\mathbf{n}$ and $\mathbf{n}$ is a unit vector, one can further express these derivatives as

$$u_{,\tau_i} = \boldsymbol{\nu}_\mathbf{i}\cdot\boldsymbol{\omega}_\mathbf{i} - \mathbf{b}\boldsymbol{\tau}_\mathbf{i}\cdot\mathbf{u}, \tag{28}$$

and

$$u_{,\nu_i} = -\boldsymbol{\tau}_\mathbf{i}\cdot\boldsymbol{\omega}_\mathbf{i} - \mathbf{b}\boldsymbol{\nu}_\mathbf{i}\cdot\mathbf{u}, \tag{29}$$

where $\boldsymbol{\omega}_i$ is a vector associated with the variation of the surface normal that satisfies the relation $\dot{\mathbf{n}}_i = \boldsymbol{\omega}_i \times n_i$. '$i$' refers to a specific membrane domain and its multiple occurrence in a mathematical expression should not be interpreted to imply summation over i.

With the substitution of the above equations, (26) can be expressed in the compact form [19]

$$\dot{E}^i_B = \int_{\partial\omega_i} (F^i_\nu \boldsymbol{\nu}_i + F^i_\tau \boldsymbol{\tau}_i + F^i_n \mathbf{n}_i)\cdot\mathbf{u}\, ds - \int_{\partial\omega_i} M^i \boldsymbol{\tau}_i\cdot\boldsymbol{\omega}_i\, ds, \tag{30}$$

where

$$M^i = \tfrac{1}{2}W^i_H + \kappa^i_\tau W^i_K, \tag{31}$$

and

$$F^i_\nu = W^i + \lambda_i - \kappa^i_\nu M^i, \quad F^i_\tau = -\tau^i M^i, \quad \text{and} \quad F^i_n = (\tau^i W^i_K)_{,\tau_i} - \left(\frac{1}{2}W^i_H\right)_{,\nu_i} - (W^i_K)_{,\beta}\tilde{b}^{\alpha\beta}\nu^i_\alpha. \tag{32}$$

Above, M^i is the bending couple per unit length and F^i_ν, F^i_τ and F^i_n are the forces per unit length in the $\boldsymbol{\nu}_i$, $\boldsymbol{\tau}_i$ and $\mathbf{n}_i$ direction, respectively, that act at the boundary.

3.2. Contact domain

In order to compute the variation of E_c, we first calculate the variation of the adhesion energy E_a. To this end, we first treat the contact domain as a material surface. The associated variations do not belong to the most general class and hence furnish necessary conditions that an energy minimizing state must respect. We resort to the procedure adopted in Section 2 that yields

$$\dot{E}_a = -\int_{\omega_c} \sigma(\theta^\alpha)(\dot{J}/J)\, da. \tag{33}$$

For tangential variations, using $(18)_1$, and the Stokes' theorem we obtain

$$(\dot{E}_a)_t = \int_{\omega_c} u^\alpha \sigma_{,\alpha}\, da - \int_{\partial\omega_c} \sigma u^\alpha \nu^c_\alpha\, ds. \tag{34}$$

Employing $(22)_1$, the normal variations yield

$$(\dot{E}_a)_n = \int_{\omega_c} 2\sigma H u\, da. \tag{35}$$

Summing (34) and (35), we obtain the total variation of the adhesion energy

$$\dot{E}_a = \int_{\omega_c} (u^\alpha \sigma_{,\alpha} + 2\sigma H u)\, da - \int_{\partial\omega_c} \sigma u^\alpha \nu^c_\alpha\, ds. \tag{36}$$

First, we evaluate the tangential variation of the energy E_c of the contact domain. Invoking Equations (19) and (20) for the two membrane surfaces in the adhered region ω_c and (34) for the adhesion energy one obtains

$$(\lambda_c - \sigma)_{,\alpha} = -\partial W^c / \partial \theta^\alpha, \tag{37}$$

where

$$W^c = W^1 + W^2 \quad \text{and} \quad \lambda_c = \lambda_1 + \lambda_2 \tag{38}$$

are the total bending energy and the surface tension of the adhered domain, respectively. From (37), it can be seen that a spatial variation in the strength of adhesion leads to a change in the surface tension field. Similarly, for the normal variations, employing (24) for the two apposing membranes and (35) for the adhesion energy together furnish the shape equation for the adhered domain

$$\Delta(\tfrac{1}{2} W^c_H) + (W^c_K)_{;\beta\alpha} \tilde{b}^{\beta\alpha} + W^c_H (2H^2 - K) + 2KHW^c_K - 2H(W^c + \lambda_c - \sigma) = p_c, \tag{39}$$

where $p_c = p_1 + p_2$. Comparing the last term on the left-hand side of (39) with that of (25) for a single membrane, $\lambda_c - \sigma$ can be interpreted as the apparent surface tension in the adhered regime.

With the Euler equations satisfied in the domain ω_c, variation of the energy functional (14) reduces to the boundary term

$$\dot{E}^c_B = \int_{\partial\omega_c} (F^c_\nu \boldsymbol{\nu}_c + F^c_\tau \boldsymbol{\tau}_c + F^c_n \mathbf{n}_c) \cdot \mathbf{u}\, ds - \int_{\partial\omega_c} M^c \boldsymbol{\tau}_c \cdot \boldsymbol{\omega}_c\, ds, \tag{40}$$

where

$$M^c = \tfrac{1}{2} W^c_H + \kappa^c_\tau W^c_K \tag{41}$$

and

$$F^c_\nu = W^c + \lambda_c - \sigma - \kappa^c_\nu M^c, \quad F^c_\tau = -\tau^c M^c \quad \text{and} \quad F^c_n = (\tau^c W^c_K)_{,\tau_c} - \left(\tfrac{1}{2} W^c_H\right)_{,\nu_c} - (W^c_K)_{,\beta} \tilde{b}^{\alpha\beta} \nu^c_\alpha, \tag{42}$$

where $\boldsymbol{\nu}_c$ is the outward normal and $\boldsymbol{\tau}_c$ is the tangent associated with the contact boundary.

Next, we consider variations of the contact boundary that allow the material points to move into and out of the adhered domain. Such variations have previously been considered in the context of membrane–substrate adhesion [19]. As the set of material points in the adhered domain is allowed to evolve, there is a lack of one-to-one correspondence between a point in the reference configuration and a point in the deformed configuration. As a consequence, an operation like material time derivative is not defined and the variational derivative that we considered in the previous sections, which behaves similar to a material time derivative, is not operative. For such variations, one can resort to a geometrical approach with arbitrary infinitesimal variations $\mathbf{u}$ associated with the contact boundary. Projection of the virtual displacements in the direction of the exterior normal $\boldsymbol{\nu}_c$ to the boundary and multiplication with the length of a small segment with arclength ds yields the infinitesimal

change in the area $da = \boldsymbol{\nu}_c \cdot \mathbf{u}\, ds$ up to the first order. Integration of this areal change over the entire boundary furnishes the net change in the adhesion energy [19]

$$\dot{E}_a = -\int_{\partial\omega_c} \sigma u^\alpha \nu_\alpha^c \, ds. \tag{43}$$

In contrast to (36), the variation in (43) only has a boundary term. This is expected as the change in the adhesion energy is decoupled from the stretching of the membrane surface. On incorporating (43) into the variation of E_c, we recover the boundary working terms (40)–(42). The difference between the current variation and the previous variation is restricted to the shape equation in the adhered domain. For the current variation, there is no contribution from the adhesion energy towards the apparent surface tension. If the surface area of the membranes is conserved, which in general is a valid assumption, this is of no consequence as the surface tension is a Lagrange multiplier and will assume any value that may be necessary to impose the constraint and maintain equilibrium.

3.3. Interface conditions

For the two free domains $\tilde{\omega}_1$ and $\tilde{\omega}_2$, the exterior normals point in a direction opposite to that of the contact domain. Thus, $\boldsymbol{\nu}_1 = -\boldsymbol{\nu}_c$ and $\boldsymbol{\nu}_2 = -\boldsymbol{\nu}_c$. Therefore, derivatives along $\boldsymbol{\nu}_1$, $()_{,\nu_1}$, and along $\boldsymbol{\nu}_2$, $()_{,\nu_2}$, satisfy the relation $(\,)_{,\nu_1} = (\,)_{,\nu_2} = -(\,)_{,\nu_c}$. As the surface normals are assumed to be continuous everywhere and aligned in the same direction, $\mathbf{n}_1 = \mathbf{n}_2 = \mathbf{n}_c$ at the interface. Since $\boldsymbol{\tau} = \mathbf{n} \times \boldsymbol{\nu}$, it follows that $\boldsymbol{\tau}_1 = -\boldsymbol{\tau}_c$ and $\boldsymbol{\tau}_2 = -\boldsymbol{\tau}_c$. This further implies that arclength derivatives along $\boldsymbol{\tau}_1$, $(\,)_{,\tau_1}$, or $\boldsymbol{\tau}_2$, $(\,)_{,\tau_2}$, satisfy the relation $(\,)_{,\tau_1} = ()_{,\tau_2} = -(\,)_{,\tau_c}$. Furthermore, it can be shown that $\boldsymbol{\tau} \cdot \boldsymbol{\omega} = -\mathbf{n} \cdot \mathbf{u}_{,\nu}$ [19], which yields the relation $\boldsymbol{\tau}_1 \cdot \boldsymbol{\omega}_1 = \boldsymbol{\tau}_2 \cdot \boldsymbol{\omega}_2 = -\boldsymbol{\tau}_c \cdot \boldsymbol{\omega}_c$ at the interface.

Taking the above discussion into consideration and adding the contributions from (30) and (40) we obtain the total residual working associated with the interface $\partial\omega_c$

$$\dot{E}_B = \int_{\partial\omega_c} (P_\nu \boldsymbol{\nu}_c + P_\tau \boldsymbol{\tau}_c + P_n \mathbf{n}_c) \cdot \mathbf{u}\, ds - \int_{\partial\omega_c} Q \boldsymbol{\tau}_\mathbf{c} \cdot \boldsymbol{\omega}_c \, ds, \tag{44}$$

where

$$P_\nu = F_\nu^c - F_\nu^1 - F_\nu^2 = [F_\nu^1 + F_\nu^2] - \sigma, \tag{45}$$

$$P_\tau = F_\tau^c - F_\tau^1 - F_\tau^2 = [F_\tau^1 + F_\tau^2], \tag{46}$$

$$P_n = F_n^c - F_n^1 - F_n^2 = [F_n^1 + F_n^2], \tag{47}$$

and

$$Q = M^c - M^1 - M^2 = [M^1 + M^2]. \tag{48}$$

Here and henceforth, we define and use the notation $[(\,)] = (\,)_c - (\,)_f$, where c and f refer to the limits as the boundary $\partial\omega_c$ is approached from the adhered and the free sides. Furthermore, quantities associated with either superscripts or subscripts $\{1, 2\}$ that are not enclosed in [ ] are evaluated in the free domain $\tilde{\omega}_i$ at the interface.

We consider equilibrium solutions where the position field $\mathbf{r}(\theta^\mu)$ is piecewise continuous in the sense that it admits discontinuities in the second derivatives $\mathbf{r}_{,\alpha\beta}$. Such states allow for jumps in the curvatures and are of the form [20, 21]

$$[\mathbf{r}_{,\alpha\beta}] = \mathbf{a}\, \nu_\alpha \nu_\beta \tag{49}$$

for some three-vector $\mathbf{a}$. From (49) we can conclude that

$$[\kappa_\tau] = [\tau] = 0. \tag{50}$$

Thus, the normal curvature in the tangential direction and the twist associated with an arbitrary curve lying on a surface are always continuous. In the present context, this implies that at the boundary of the adhered domain $\partial\omega_c$

$$\kappa_\tau^c = \kappa_\tau^1 = \kappa_\tau^2 \quad \text{and} \quad \tau^c = \tau^1 = \tau^2. \tag{51}$$

First, we consider variations that induce rotation around the contact edge with vanishing translations at the interface. This is tantamount to the requirement that $\mathbf{u} = \mathbf{0}$ but $\boldsymbol{\tau}_{\mathbf{c}} \cdot \boldsymbol{\omega}_c = -\mathbf{n}_c \cdot \mathbf{u}_\nu$ is arbitrary at the interface. It bears emphasis that $\mathbf{u}$ and $\mathbf{u}_\nu$ can be varied independently at the contact boundary [22]. For such a class of variations the stationarity condition reduces to

$$\int_{\partial\omega_c} Q\boldsymbol{\tau}_{\mathbf{c}} \cdot \boldsymbol{\omega}_c ds = 0. \tag{52}$$

Since $\mathbf{u}_\nu$ is arbitrary, (52) implies

$$Q = 0. \tag{53}$$

Substituting (31), (41) and (48) in (53) furnishes the first jump condition

$$\frac{1}{2}[W_H^1 + W_H^2] + \kappa_\tau^c[W_K^1 + W_K^2] = 0. \tag{54}$$

Next, we consider variations in the tangential plane such that $\boldsymbol{\nu}_c \cdot \mathbf{u} = 0$. With (53) satisfied, the stationarity condition reduces to

$$\int_{\partial\omega_c} P_\tau \boldsymbol{\tau}_{\mathbf{c}} \cdot \mathbf{u} ds = 0 \tag{55}$$

which yields

$$P_\tau = 0. \tag{56}$$

Combining $(32)_2$, $(42)_2$, (46), (48) and (51) we obtain

$$P_\tau = -\tau^c[M^1 + M^2] = -\tau^c Q. \tag{57}$$

Since (53) requires Q to vanish at the contact boundary, (56) is trivially satisfied. Next, we consider pure normal variations with $\boldsymbol{\tau}_c \cdot \mathbf{u} = 0$ and $\boldsymbol{\nu}_c \cdot \mathbf{u} = 0$. Invoking (53), the energy variation reduces to

$$\int_{\partial\omega_c} P_n \mathbf{n} \cdot \mathbf{u} ds = 0. \tag{58}$$

Using (47), (58) yields

$$[F_n^1 + F_n^2] = 0. \tag{59}$$

Substituting $(42)_3$ and $(32)_3$ in (59) furnishes the second jump condition

$$[\{\tau^c(W_K^1 + W_K^2)\}_{,\tau_c} - \frac{1}{2}(W_H^1 + W_H^2)_{,\nu_c} - (W_K^1 + W_K^2)_{,\beta}\tilde{b}^{\alpha\beta}\nu_\alpha^c] = 0. \tag{60}$$

In the above equation, $\bar{b}^{\alpha\beta}$ needs to be evaluated separately for the two surfaces. Finally, we consider divergence-free tangential variations that satisfy $\int_{\partial\omega_c} \mathbf{u} \cdot \boldsymbol{\nu}_c ds = 0$. For such variations stationarity requires (see [19] for details)

$$\int_{\partial\omega_c} Q_\nu \boldsymbol{\nu}_{\mathbf{c}} \cdot \mathbf{u} ds = 0, \tag{61}$$

where $Q_\nu = [Q_\nu^1 + Q_\nu^2] - \sigma, Q_\nu^1 = W^1 - k_\nu^1 M^1$, and $Q_\nu^2 = W^2 - k_\nu^2 M^2$. (61) then implies

$$[Q_\nu^1 + Q_\nu^2] = \sigma \tag{62}$$

which furnishes the final jump condition

$$[W^1 + W^2] - [k_\nu^1(\tfrac{1}{2}W_H^1) + k_\nu^2(\tfrac{1}{2}W_H^2)] - k_\tau^c[k_\nu^1 W_K^1 + k_\nu^2 W_K^2] = \sigma. \tag{63}$$

In summary, for the case of two membranes that adhere to each other, we obtain three jump conditions at the contact boundary. These are associated with the balance of traction forces along the normal to the surface, normal to the boundary in the tangent plane, and the bending moment at the interface. In contrast, for the case of membrane–substrate adhesion, equilibrium considerations yielded a single jump condition associated with the normal force F_ν at the boundary. The jump conditions (54), (60), and (63) derived above entertain the most general type of strain energy associated with fluid surfaces.

4. Helfrich energy

In this section, we specialize the aforementioned results for the case of membranes with a strain energy quadratic in curvature, popularly known as the Helfrich energy. These are of the form

$$W = k(H - C)^2 + \bar{k}K, \tag{64}$$

where C is the spontaneous curvature, and k and $\bar{k}$, respectively, are the moduli associated with the mean and the Gaussian curvature. The first constant, k, is commonly referred to as the bending modulus. From (64), we compute

$$\tfrac{1}{2}W_H = k(H - C), \quad W_K = \bar{k}. \tag{65}$$

First, we specialize the jump conditions at the interface. Substitution of (65) into (54) yields

$$[k_1(H_1 - C_1) + k_2(H_2 - C_2)] + \kappa_\tau^c[\bar{k}_1 + \bar{k}_2] = 0, \tag{66}$$

where $\{k_1, \bar{k}_1\}$ and $\{k_2, \bar{k}_2\}$ are the moduli associated with the two bilayers. Similarly, $\{H_1, C_1\}$ and $\{H_2, C_2\}$ are the mean curvatures and the spontaneous curvatures of the two bilayers. If the moduli and the spontaneous curvature are assumed to be uniform everywhere, Equation (66) reduces to

$$k_1H_1 + k_2H_2 = (k_1 + k_2)H_c. \tag{67}$$

Here H_1, H_2 and H_c are the mean curvatures of $\tilde{\omega}_1$, $\tilde{\omega}_2$ and ω_c, respectively, at the interface. With the help of (4) and (51), Equation (67) can also be expressed in terms of the normal curvatures κ_ν as

$$k_1\,\kappa_\nu^1 + k_2\,\kappa_\nu^2 = (k_1 + k_2)\kappa_\nu^c. \tag{68}$$

In the second jump condition given by (60), the third terms drop out as W_K is a constant. This along with the fact that twist τ^c and its tangential derivative are continuous fields reduce (60) to

$$[k_1(H_1 - C_1)_{,\nu_c} + k_2(H_2 - C_2)_{,\nu_c}] = 0. \tag{69}$$

For uniform bending moduli and spontaneous curvatures, Equation (69) simplifies to

$$k_1(H_1)_{,\nu_c} + k_2(H_2)_{,\nu_c} = (k_1 + k_2)(H_c)_{,\nu_c}. \tag{70}$$

Using (4) and the continuity of κ_τ at the interface, Equation (70) can further be expressed as

$$k_1(\kappa_\nu^1)_{,\nu_c} + k_2(\kappa_\nu^2)_{,\nu_c} = (k_1 + k_2)(\kappa_\nu^c)_{,\nu_c}. \tag{71}$$

Finally, substituting (64) and (65) into (63), one obtains

$$[k_1(H_1 - C_1)^2 + k_2(H_2 - C_2)^2] - 2[k_1H_1(H_1 - C_1) + k_2H_2(H_2 - C_2)] = \sigma. \tag{72}$$

For the case of continuous bending moduli and spontaneous curvatures, Equation (72) reduces to

$$k_1H_1^2 + k_2H_2^2 = (k_1 + k_2)H_c^2 + \sigma. \tag{73}$$

Again, making use of (4) and the fact that $[\kappa_\tau] = 0$, Equation (73) can be shown to be equivalent to

$$k_1(\kappa_\nu^1)^2 + k_2(\kappa_\nu^2)^2 - (k_1 + k_2)(\kappa_\nu^c)^2 = 4\sigma. \tag{74}$$

The interface conditions (68), (71) and (74) match with those obtained by Muller et al. [6] for membranes with vanishing spontaneous curvature. It is interesting to note that a uniform spontaneous curvature in the membranes has no influence on the interface conditions. However, if the membrane properties such as bending

moduli or spontaneous curvature vary spatially either due to adhesion or due to other biochemical interactions, the appropriate jump conditions are given by (66), (69) and (72).

The equilibrium shape of the three membrane domains is given by the shape equations (25) and (39). For the Helfrich energy with piecewise uniform spontaneous curvature in the three domains, these respectively reduce to

$$k_i\Delta(H) + 2k_i(H - C_i)(2H^2 - K) - 2k_iH(H - C_i)^2 = p_i + 2\lambda_iH, \tag{75}$$

and

$$(k_1+k_2)\Delta H+2\{k_1(H-C_1)+k_2(H-C_2)\}(2H^2-K)-2H\{k_1(H-C_1)^2+k_2(H-C_2)^2\} = p_c+2(\lambda_c-\sigma)H. \tag{76}$$

It should be noted that in order to maintain clarity, we have refrained from the use of subscripts i and c for geometric variables H and K in the Euler–Lagrange equations. They should be interpreted in the context of the domain under consideration. As we restrict ourselves to membranes with uniform properties in the three domains, Equations (21) and (37) imply that the surface tensions λ_1, λ_2 and λ_c assume constant values in all the domains.

5. Examples: vesicle–vesicle adhesion

We employ the equilibrium equations discussed in the previous section to simulate vesicle–vesicle adhesion. The two lipid bilayers under isolated conditions are assumed to possess vanishing spontaneous curvature. However, we allow for the possibility that the adhesion molecules can generate a preferential curvature in the membranes in the adhered domain. We restrict ourselves to the equilibrium shapes that exhibit axisymmetry. Such solutions can be parametrized by meridional arclength s and azimuthal angle θ. Thus, the position vector

$$\mathbf{r}(s, \theta) = r(s)\mathbf{e}_r(\theta) + z(s)\mathbf{k}, \tag{77}$$

where $r(s)$ is the radial distance from the axis of symmetry and $z(s)$ is the height with respect to a fixed datum. We choose $\theta^1 = s$ and $\theta^2 = \theta$. As s measures the arclength along a meridian, given by a curve with constant θ, $(r')^2 + (z')^2 = 1$, where $(\,)' = d(\,)/ds$. This implies that there exists a $\psi(s)$ such that

$$r'(s) = \cos\psi \quad \text{and} \quad z'(s) = \sin\psi. \tag{78}$$

Using the relations outlined in Section 1, the metric and dual metric can be obtained as $(a_{\alpha\beta}) = \mathrm{diag}(1, r^2)$ and $(a^{\alpha\beta}) = \mathrm{diag}(1, r^{-2})$, respectively. From Equation (1), the covariant components of the curvature tensor can be calculated to be $(b_{\alpha\beta}) = \mathrm{diag}(\psi', r\sin\psi)$. Combining these results with (3), furnishes

$$\kappa_\nu = \psi', \quad \kappa_\tau = r^{-1}\sin\psi \quad \text{and} \quad \tau = 0. \tag{79}$$

Employing the definitions of the mean curvature and the Gaussian curvature we obtain

$$r\psi' = 2rH - \sin\psi, \tag{80}$$

and

$$K = H^2 - (H - r^{-1}\sin\psi)^2. \tag{81}$$

The shape equations (75) and (76) simplify to

$$L' = r[(p_i/k_i) + (2\lambda_i/k_i)H - 2H(H - r^{-1}\sin\psi)^2], \tag{82}$$

and

$$L' = r[(p_c/(k_1 + k_2)) + 2(\lambda_c - \sigma)H/(k_1 + k_2) - 2(H - C_0)\{H^2 + (H - r^{-1}\sin\psi)^2\} + 2H(H - C_0)^2], \tag{83}$$

where

$$H' = r^{-1}L, \tag{84}$$

and C_0 is the uniform spontaneous curvature in the two bilayers in the contact domain possibly induced by the adhesion molecules. (78), (80), (82), (83), and (84) constitute the set of governing differential equations that are required to be integrated along with the appropriate boundary conditions and the jump conditions to obtain an equilibrium configuration. Interface conditions (67) and (73) can be used in their original form but (70) needs some rearrangement. Using (84) and the relation $(\,)' = (\,)_{,\nu_c}$, we express the derivative of the mean curvature in (70) in terms of the new variables L. This along with the continuity of the position vector yield the modified form of (70)

$$k_1 L_1 + k_2 L_2 = (k_1 + k_2) L_c. \tag{85}$$

In order to simulate the response of vesicles with constrained area, we change the independent variables from arclength s to area a. To this end, we use the expression of the area of a sector on a solid of revolution given by

$$a(s) = 2\pi \int_0^s r(t)\, dt. \tag{86}$$

This yields $a'(s) = 2\pi r(s)$. Since $r(s) > 0$, a is strictly positive and the choice of a as the independent variable is justified. The areal constraint is then simply enforced by integrating the system of governing equations on a fixed domain. Furthermore, we non-dimensionalize the equations with the radius R of a sphere that has the same surface area as the bigger of the two vesicles. This yields the dimensionless variables

$$\begin{aligned} &\alpha = a/(2\pi R^2), \quad x = r/R, \quad y = z/R, \quad h = RH, \quad c_0 = RC_0, \quad l = RL, \quad \bar{\lambda}_i = R^2\lambda_i/k_i, \\ &\bar{\lambda}_c = R^2\lambda_c/(k_1 + k_2), \quad \bar{\sigma} = R^2\sigma/(k_1 + k_2), \quad \bar{p}_i = p_i R^3/k_i, \quad \text{and} \quad \bar{p}_c = p_c R^3/(k_1 + k_2). \end{aligned} \tag{87}$$

In terms of these variables, the differential equations take the form

$$x\dot{x} = \cos\psi, \quad x\dot{z} = \sin\psi, \quad x^2\dot{\psi} = 2xh - \sin\psi, \quad x^2\dot{h} = l, \tag{88}$$

$$\dot{l} = \bar{p}_i + 2h[\bar{\lambda}_i - (h - x^{-1}\sin\psi)^2], \tag{89}$$

and

$$\dot{l} = \bar{p}_c + 2h[\bar{\lambda}_c - \bar{\sigma} - 2(h - c_0)\{h^2 + (h - x^{-1}\sin\psi)^2\} + 2h(h - c_0)^2], \tag{90}$$

where $(\cdot)^{\cdot} = d(\cdot)/d\alpha$. The three interface conditions (66), (72) and (85) change to

$$k_1 h_1 + k_2 h_2 = (k_1 + k_2)(h_c - c_0), \quad k_1 h_1^2 + k_2 h_2^2 = (k_1 + k_2)(h_c^2 - c_0^2 + \bar{\sigma}) \quad \text{and} \quad k_1 l_1 + k_2 l_2 = (k_1 + k_2) l_c. \tag{91}$$

First we discuss the equilibrium shapes of two identical vesicles adhered to each other. The induced spontaneous curvature c_0 is assumed to be zero. The problem has both rotational symmetry about the vertical axis $\mathbf{k}$ and reflection symmetry about the horizontal plane containing the contact domain. The reflection symmetry requires the contact domain to remain planar and as a consequence $h_c = 0$, $l_c = 0$. Since the two vesicles have equal and opposite curvatures, Equations $(91)_1$ and $(91)_3$ are trivially satisfied. Equation $(91)_2$ simplifies to $h_1^2 = h_2^2 = \bar{\sigma}$ and yields $h_1 = -h_2 = -\sqrt{\bar{\sigma}}$. At a first glance this relation looks the same as that for a vesicle adhering to a planar substrate as discussed in [19]. However, it should be noted that the definition of the normalized adhesion energy differs for the two cases. For vesicle–vesicle adhesion $\bar{\sigma} = R^2\sigma/2k$, whereas for vesicle–substrate adhesion $\bar{\sigma} = R^2\sigma/k$ (see [19]). This implies that for a given adhesion energy σ, the effective adhesion is greater by a factor of two for a vesicle interacting with a substrate than with an identical vesicle. This point has also been highlighted in [6]. The solution of a vesicle adhering to a planar substrate [19] can therefore be adapted to obtain the equilibrium shapes of adhered identical vesicles.

We now consider adhesion between two vesicles of different sizes. We assume $k_1 = k_2$ and $c_0 = 0$. In contrast to the case of identical vesicles, this problem lacks reflection symmetry. Thus, the contact domain can curve and possess a non-vanishing mean curvature. As a result, the differential equations have to be integrated over the contact domain and the two free domains. This results in a four-point boundary value problem that is subjected to the jump conditions in (91) and the continuity conditions for the position vector and the tangent vector. This constitutes a more general class of problems than that modeled by Derganc et al. [11] where the

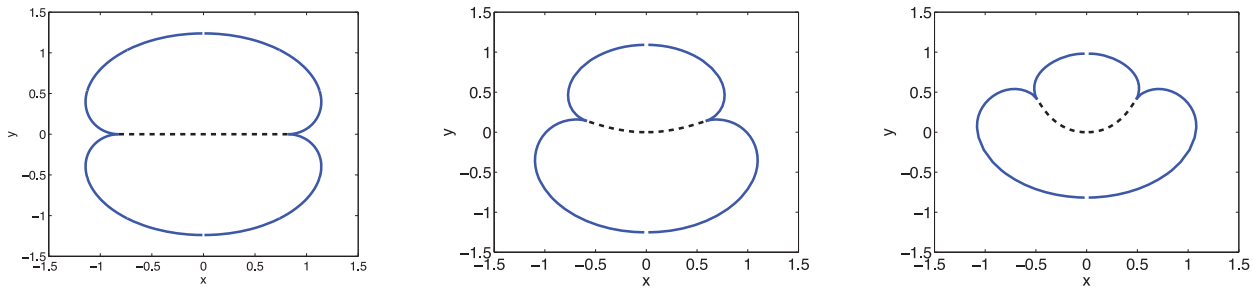

Figure 3. Effect of relative sizes on the shapes of adhered vesicles ($\bar{\sigma} = 4$): (a) $a_r = 1$, (b) $a_r = 0.49$ and (c) $a_r = 0.25$.

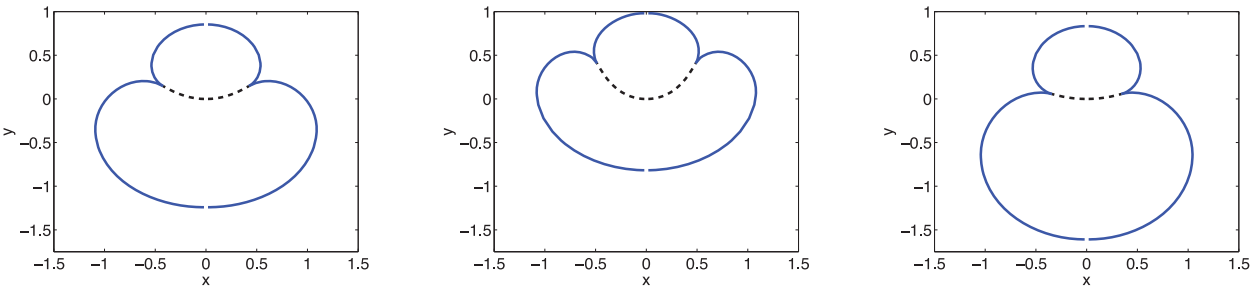

Figure 4. Effect of internal pressures on the shapes of adhered vesicles ($a_r = 0.25$, $\bar{\sigma} = 4$): (a) $\bar{p}_1 = 0, \bar{p}_2 = -2$; (b) $\bar{p}_1 = 0, \bar{p}_2 = 0$; and (c) $\bar{p}_1 = 3, \bar{p}_2 = 0$. Subscript '1' corresponds to the lower vesicle and '2' corresponds to the upper one.

integration was carried out over two domains due to periodic boundary conditions. Let α_c, α_1 and α_2 correspond to the normalized areas of the adhered domain and the two vesicles. Then, to obtain the equilibrium shapes (90) is integrated over the domain $[0, \alpha_c]$, and (89) is integrated over the domains $[\alpha_c, \alpha_1]$ and $[\alpha_1, \alpha_2]$. We define a_r as the ratio of the surface area of the smaller vesicle to that of the bigger vesicle. Figure 3(a), 3(b) and 3(c) shows the adhered morphology of vesicles with $a_r = 1.00$, 0.49 and 0.25, respectively, for $\bar{\sigma} = 4$ and vanishing osmotic pressures. As can be observed, an increase in the disparity between the vesicle sizes leads to an increase in the degree to which the bigger vesicle wraps around the smaller vesicle.

Next, we model the effect of internal pressure on the equilibrium shapes of two adhered vesicles with $k_1 = k_2$, $c_0 = 0$, and $a_r = 0.25$. The results are shown in Figure 4. First we increase the internal pressure in the smaller vesicle ($\bar{p}_1 = 0$ and $\bar{p}_2 = -2$). This results in a reduced wrapping of the smaller vesicle by the bigger vesicle (Figure 4(a)). Next, the internal pressure in the larger vesicle is increased ($\bar{p}_1 = 3$ and $\bar{p}_2 = 0$) which leads to a similar reduction in the engulfment of the smaller vesicle by the larger vesicle (Figure 4(c)). As could be expected, a non-zero internal pressure in a vesicle decreases its deformability or compliance reducing the level of adhesion-induced deformations. This highlights the role of the surface area to volume ratio in governing the physical interactions between vesicles with constrained volume. It agrees with the common experimental practice where the adhesion of vesicles with substrates and other vesicles is achieved by changing the concentration of the buffer solution. An increase in the surface area to volume ratio of the originally spherical vesicles facilitates adhesion.

Finally, we consider the possibility that the adhesion molecules can generate a spontaneous curvature in the two bilayers. This effect is localized to the contact domain. We model vesicle shapes with $k_1 = k_2$, $a_r = 0.49$ for three values of induced curvature, $c_0 = -0.5$, $c_0 = 0$ and $c_0 = 0.1$. The results are shown in Figure 5. It can be observed that a negative curvature reduces the degree to which the bigger vesicle wraps the smaller

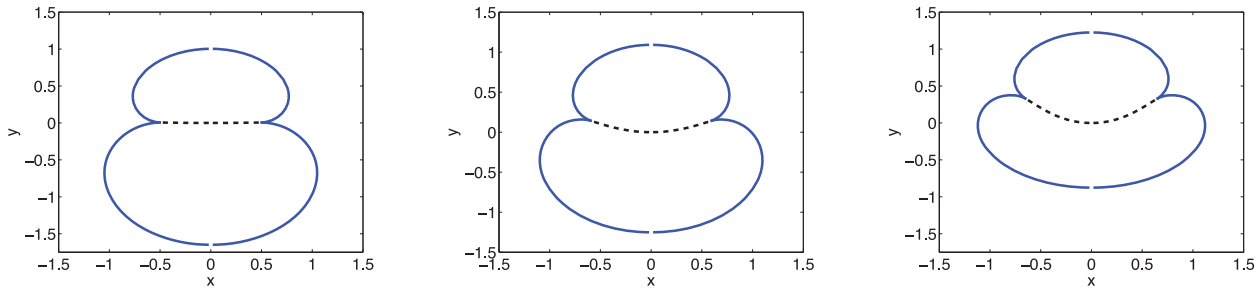

Figure 5. Effect of adhesion-induced spontaneous curvature on the shapes of adhered vesicles ($a_r = 0.49$, $\bar{\sigma} = 4$): (a) $c_0 = -0.5$, (b) $c_0 = 0$ and (c) $c_0 = 0.1$.

vesicle. Furthermore, it is interesting to note that the effect of the spontaneous curvature is such that the contact domain assumes a planar configuration. In contrast, a negative induced curvature increases the extent to which the bigger vesicle wraps around the smaller vesicle. In addition, it should be noted that a small deviation from zero spontaneous curvature towards negative values can significantly impact the degree of wrapping.

As shown above, the generalized framework presented in the earlier sections can be used to model adhesion between vesicles with localized variations in the membrane properties. Such a model can be employed to study the uptake of liposomes by cells and aggregation of erythrocytes with different mechanical properties that do not necessarily form periodic structures. Such investigations will be the subject of future studies.

Funding

This research received no specific grant from any funding agency in the public, commercial, or not-for-profit sectors.

Conflict of Interest

None declared.

Acknowledgements

The majority of this work was carried out during the author's stay at the University of Houston. The author thanks Professor David Steigmann for insightful discussions.

References

[1] Seifert, U, and Lipowsky, R. Adhesion of vesicles. *Phys Rev A* 1990; 42: 4768–4771.
[2] Rosso, R, and Virga, EG. Adhesion by curvature of lipid tubules. *Continuum Mech Thermodyn* 1998; 10: 359–367.
[3] Capovilla, R, and Guven, J. Geometry of lipid vesicle adhesion. *Phys Rev E* 2002; 66: 041604.
[4] Müller, MM, Deserno, M, and Guven, J. Geometry of surface-mediated interactions. *Europhys Lett* 2005; 69: 482–488.
[5] Deserno, M, Müller, MM, and Guven, J. Contact lines for fluid surface adhesion. *Phys Rev E* 2007; 76: 011605.
[6] Müller, MM, Deserno, M and Guven, J. Balancing torques in membrane-mediated interactions: Exact results and numerical illustrations. *Phys Rev E* 2007; 76: 011921.
[7] Feng, XQ, Shi, W, and Gao, H. Two-dimensional model of vesicle adhesion on curved substrates. *Acta Mech Sinica* 2006; 22: 529–535.
[8] Das, S, and Du, Q. Adhesion of vesicles to curved substrates. *Phys Rev E* 2008; 77: 011907.
[9] Alberts, B, Johnson, A, Lewis, J, Raff, M, Roberts, K, and Walter, P. *Molecular Biology of the Cell*. New York: Garland Science, 2002.
[10] Evans, EA. Detailed mechanics of membrane–membrane adhesion and separation. i. continuum of molecular cross-bridges. *Biophys J* 1985; 48: 175–183.
[11] Derganc, J, Bozic, B, Svetina, S, and Zeks, B. Equilibrium shapes of erythrocytes in rouleau formation. *Biophys J.* 2003; 84: 1486–1492.

[12] Ziherl, P, and Svetina, S. Flat and sigmoidally curved contact zones in vesicle-vesicle adhesion. *Proc Natl Acad Sci U S A* 2007; 104: 761–765.
[13] Brakke, K. *Surface evolver*. http://www.susqu.edu/facstaff/b/brakke/evolver/evolver.html.
[14] Lipowsky, R. Flexible membranes with anchored polymers. *Coll Surf A: Physicochem Eng Aspects* 1997; 128: 255–264.
[15] Steigmann, DJ. Fluid films with curvature elasticity. *Arch Rational Mech Anal* 1999; 150: 127–152.
[16] Steigmann, DJ, Baesu, E, Rudd, RE, Belak, J, and McElfresh, M. On the variational theory of cell–membrane equilibria. *Interfaces Free Boundaries* 2003; 5: 357–366.
[17] Agrawal, A, and Steigmann, DJ. Modeling protein-mediated morphology in biomembranes. *Biomech Modeling Mechanobiol* 2009; 8: 371–379.
[18] Ou-Yang, Z-C, Liu, J-X, and Xie, Y-Z. *Geometric Methods in the Elastic Theory of Membranes in Liquid Crystal Phases*. Singapore: World Scientific, 1999.
[19] Agrawal, A, and Steigmann, DJ. Boundary-value problems in the theory of lipid membranes. *Continuum Mech Thermodyn* 2009; 21: 57–82.
[20] Hilgers, MG, and Pipkin, AC. Energy-minimizing deformations of elastic sheets with bending stiffness. *J Elasticity* 1993; 31: 125–139.
[21] Agrawal, A, and Steigmann, DJ. Coexistent fluid-phase equilibria in biomembranes with bending elasticity. *J Elasticity* 2008; 93: 63–80.
[22] Landau, LD, and Lifschitz, EM. *Theory of Elasticity, 3rd edn. Vol. 7 of the Course of Theoretical Physics*. Pergamon, 1986.